

## The Ethene–Ozone Reaction in the Gas Phase

Peter Neeb,\* Osamu Horie, and Geert K. Moortgat

Max-Planck-Institut für Chemie, Division of Atmospheric Chemistry, P.O. Box 3060, D-55020 Mainz, Germany

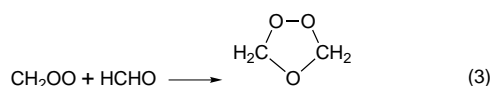
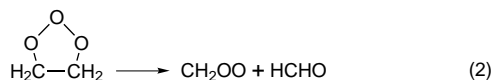
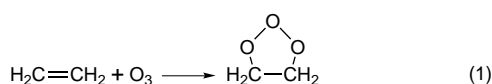
Received: February 24, 1998; In Final Form: June 1, 1998

The ethene–ozone reaction was investigated in a 570 L spherical glass reactor at atmospheric pressure, using long-path FTIR spectroscopy for detection of the individual products. Experiments were performed in the presence of hydroxy and carbonyl compounds to identify the reactions of the Criegee intermediate  $\text{CH}_2\text{OO}$  formed in ethene ozonolysis. Using  $^{13}\text{C}$ -labeled  $\text{HCHO}$ , this reaction was found to proceed via an unstable cyclic adduct which decays to the detected products  $\text{HCHO}$ ,  $\text{HCOOH}$  and  $\text{CO}$ . [ $\text{CH}_2\text{OO} + \text{HCHO} \rightarrow \text{HCHO} + \text{HCOOH}$  (eq 13);  $\text{CH}_2\text{OO} + \text{HCHO} \rightarrow \text{HCHO} + \text{CO} + \text{H}_2\text{O}$  (eq 14a);  $\text{CH}_2\text{OO} + \text{HCHO} \rightarrow \text{HCHO} + \text{HCO} + \text{OH}$  (eq 14b)] The relative rates of the reactions of  $\text{CH}_2\text{OO}$  with  $\text{HCOOH}$  and  $\text{HCHO}$  were determined from the product analysis. In addition, evidence was found that the reaction of  $\text{CH}_3\text{CHO}$  with the  $\text{CH}_2\text{OO}$  intermediate does not exclusively produce secondary propene ozonide, but also  $\text{HCHO}$  and  $\text{CO}_2$ . The results of this study have been combined with data from previous investigations to give a complete description of the gas phase ozonolysis of ethene and are discussed in comparison with ozonolysis reactions occurring in the liquid phase.

### Introduction

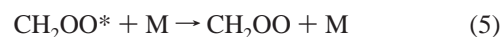
The gas phase reaction of ozone with alkenes is an important loss process for alkenes and ozone in the atmosphere. While the rate constants of  $\text{O}_3$  reactions with a variety of alkenes have been the subject of numerous studies,<sup>1</sup> the mechanisms and products are still incompletely known. Most mechanistic studies concentrated on the reaction of simple symmetric alkenes such as ethene, 2-butene, and 2,3-dimethyl-2-butene with ozone since they produce only one Criegee intermediate. The complete description of the ozonolysis of larger alkenes, e.g., isoprene or  $\beta$ -pinene is still beyond the current state of knowledge.<sup>1,2</sup>

The accepted mechanism for the reaction of ozone with ethene is based on the mechanism that was developed by Criegee<sup>3</sup> from the liquid phase investigations in the 1940s and early 1950s. The reaction is initiated by the formation of a primary ozonide (1,2,3-trioxolane) which decomposes rapidly into a Criegee intermediate (denoted as  $\text{CH}_2\text{OO}$ ) and a primary carbonyl compound (reactions 1 and 2). While the formation of the secondary ozonide (reaction 3) is the most important reaction of the Criegee intermediate in the liquid phase, its reaction pathways are quite different in the gas phase, due to the generally much lower concentrations employed and the absence of solvent molecules.



In the gas phase, a fraction of the Criegee intermediates formed in reaction 2 decompose unimolecularly (reaction 4) before they can be collisionally stabilized (reaction 5) and, after

this stabilization, can further undergo bimolecular reactions:<sup>4,5</sup>



The decomposition channels of the simplest Criegee intermediate  $\text{CH}_2\text{OO}$  have been established, based on the yield of the products  $\text{CO}_2$ ,  $\text{CO}$ ,  $\text{HCOOH}$ , and  $\text{H}_2$ , detected by FTIR spectroscopy, mass spectroscopy, or gas chromatography:<sup>4,6–8</sup>



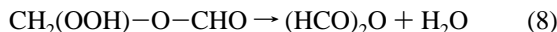
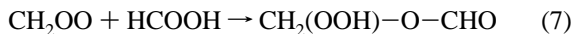
Reaction 4d proposed by Martinez et al.<sup>9</sup> is of particular interest for tropospheric chemistry, since it may serve as a light-independent source of OH radicals. Although experimental evidence supports OH radical formation,<sup>10</sup> reaction 4d has not been considered as a major decomposition channel for the excited Criegee intermediate.<sup>7,11</sup>

Compared to the decomposition pathways for the excited Criegee intermediate  $\text{CH}_2\text{OO}^*$ , less is known about the fate of the stabilized Criegee intermediate  $\text{CH}_2\text{OO}$  in the gas phase. It is known to react with aldehydes,  $\text{SO}_2$ ,  $\text{CO}$ , and  $\text{H}_2\text{O}$ <sup>5</sup> and is believed to react with  $\text{NO}$  and  $\text{NO}_2$ .<sup>12</sup> Recent studies from this laboratory have shown that the reaction of  $\text{CH}_2\text{OO}$  with hydroxylic compounds  $\text{ROH}$  proceeds in analogy to the liquid phase ozonolysis via cleavage of the hydroxylic O–H bond:<sup>13,14</sup>



During ethene ozonolysis in the presence of  $\text{HCOOH}$ , hydroperoxymethyl formate ( $\text{CH}_2(\text{OOH})-\text{O}-\text{CHO}$ , HPMF)

was formed in accordance with reaction 6 ( $R=CHO$ ).<sup>15,16</sup> HPMF is not stable in the laboratory and decomposes to formic anhydride (FAN) in a presumably heterogeneous process.<sup>4,15</sup>



Since the reported yield of HPMF<sup>4,15</sup> exceeds the reported yield of HCOOH from decomposition channel 4e at least by a factor of 4, it appears that there has to be an additional source of HCOOH in the ethene–ozone system.

Presently no reaction of the Criegee intermediate with HCHO has been formulated. In liquid phase ozonolysis the secondary ethene ozonide is formed as a major product,<sup>17</sup> but this product has not been detected so far in the gas phase, although secondary ozonides have been detected in the gas phase ozonolysis of higher alkenes by FTIR techniques and mass spectrometry.<sup>18–20</sup>

The main purpose of this study was therefore to investigate possible reactions of HCHO with the Criegee intermediate  $\text{CH}_2\text{OO}$ . Since the reaction of the Criegee intermediate with the carbonyl compound produced in the course of ozonolysis is the single most important reaction in liquid phase ozonolysis, it was hoped to point out differences and similarities in the mechanism of ozonolysis caused by the absence of solvent molecules and the much lower concentrations used in gas phase ozonolysis studies. For this purpose, a series of experiments were performed to evaluate the change of product yields, visible to FTIR spectroscopy, in the ozonolysis of ethene upon addition of HCHO,  $\text{H}^{13}\text{CHO}$ , or  $\text{CH}_3\text{CHO}$ . Together with our recent results on the reaction of the  $\text{CH}_2\text{OO}$  intermediate with hydroxylic compounds,<sup>13</sup> namely, HCOOH and  $\text{CH}_3\text{COOH}$ , a complete picture of the mechanism of the ethene ozone reaction emerges, enabling us to give some estimates for the relative rates of the reactions of the  $\text{CH}_2\text{OO}$  intermediate with HCHO and HCOOH.

## Experimental Section

Ozonolysis was carried out in  $730 \pm 3$  Torr (1 Torr = 1.333 Pa) synthetic air in an evacuable, 570 L spherical glass reactor. The reaction temperature was kept constant at  $296 \pm 2$  K by the laboratory air conditioner. Due to the large size (ca. 1 m diameter) and complex geometry, no attempts were made to vary the temperature. A schematic drawing of the reactor is shown in Figure 1. The initial reactant mixing ratios were in the range 2–9 ppmv (1 ppmv =  $2.38 \times 10^{13}$  molecule  $\text{cm}^{-3}$  at the above temperature and pressure) for  $\text{C}_2\text{H}_4$  and  $\text{O}_3$ . The mixing ratio of the added compounds ranged from 5 to 50 ppmv for HCHO and  $\text{H}^{13}\text{CHO}$  and 1–10 ppmv for HCOOH and  $\text{CH}_3\text{COOH}$ . Synthetic air was prepared by filling the reactor with 80% CO-free  $\text{N}_2$  (Linde) and 20%  $\text{O}_2$  (Linde) to a total pressure of 700–715 Torr. Ozone was generated either externally in a quartz-tube spiral surrounding a Hg Pen-ray lamp while filling the glass reactor with  $\text{O}_2$  or internally with another Hg Pen-ray lamp mounted inside the reactor. To this mixture of air and  $\text{O}_3$  premixed  $\text{C}_2\text{H}_4/\text{N}_2$  (100 ppmv  $\text{C}_2\text{H}_4$ ) from a pressurized cylinder was directly added. Also in several cases a dilute  $\text{C}_2\text{H}_4/\text{N}_2$  mixture prepared in a transfer cylinder of 1.38 L was flushed into the reactor by  $\text{N}_2$  carrier gas, until the final pressure of ca. 730 Torr was reached. During the filling, two Teflon stirrers were activated to ensure rapid mixing of the reactants. The addition of HCHO,  $\text{CH}_3\text{CHO}$ , HCOOH, and  $\text{CH}_3\text{COOH}$  was performed in a similar way, immediately before the  $\text{C}_2\text{H}_4$  injection.

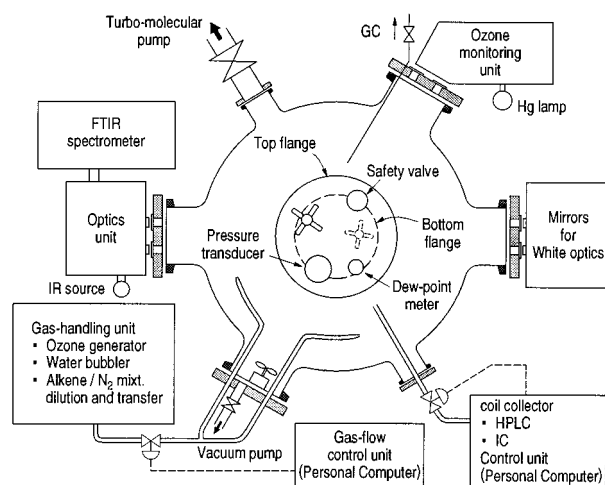


Figure 1. Schematic drawing of the 570 L glass reactor vessel.

The reactants and the products were analyzed by long-path (43.2 m path length) FTIR spectroscopy (Bruker IFS 28). For each spectrum 128 scans at a resolution of  $0.5 \text{ cm}^{-1}$  were averaged. The time resolution for the data acquisition was about 4 min at these instrumental settings. Approximate relative concentration errors were estimated as follows:  $\text{O}_3$ ,  $\text{C}_2\text{H}_4$ , CO, and HCHO  $\pm 5\%$  and  $\text{CO}_2$  and HCOOH  $\pm 10\%$ . The calibration of HCOOH was performed using a pyrolytic method<sup>21</sup> to overcome difficulties due to HCOOH dimer formation. Two different calibrations were made for HCHO which were in excellent agreement: a pyrolytic method<sup>21</sup> and a standard volumetric method using paraformaldehyde which was heated to ca.  $120 \text{ }^\circ\text{C}$  as the source for monomeric HCHO. Formic anhydride (FAN) was prepared according to the procedure of Muramatsu et al.<sup>22</sup> The reference spectrum of hydroperoxymethyl formate (HPMF) was obtained by a computational stripping procedure, and its concentration was estimated by the band strength of the carbonyl absorption.<sup>15</sup> The error limits for the concentrations of HPMF and FAN were estimated to be  $\pm 20\%$ . For  $\text{O}_3$ , the absorption cross section at  $254 \text{ nm}^{23}$  was used for its calibration.  $^{13}\text{CO}$  (IC-Chemikalien),  $\text{H}^{13}\text{COOH}$  (Aldrich), and  $\text{H}^{13}\text{CHO}$  (IC-Chemikalien) were quantified by assuming the same absorption coefficients for the corresponding peaks arising in the  $^{12}\text{C}$  compounds. Results of experiments B, H, L, and M (Table 1) have already been published in earlier studies carried out in this laboratory.<sup>13,15</sup> Reported product yields for these experiments may differ slightly from those reported in the present study, since product yields were determined at larger reaction times. Ozone concentrations have been corrected by +12% relative to previous studies due to a recalibration of the optical path length of the UV system (minor contribution) and an error in the data acquisition software (major contribution). All chemicals were of highest purity commercially available and used without further purification.

## Results

Typical FTIR spectra of the reaction mixture of the gas phase reaction of ethene with ozone are illustrated in Figure 2. Also shown in Figure 2 are parts of the reference spectra of the reactants and the products which were used to determine the concentrations listed in Table 1. Compounds quantified in this study are the educts  $\text{H}_2\text{C}=\text{CH}_2$  and  $\text{O}_3$  and the products HCHO, CO,  $\text{CO}_2$ , HCOOH, hydroperoxymethyl formate (HPMF), and formic anhydride (FAN). Results of ozonolysis experiments

**TABLE 1: Product Yields<sup>a</sup> for the Ethene–Ozone System As Determined by FTIR Spectroscopy**

	experiments in the presence of												
	A	B	C	D <sup>b</sup>	HCHO		CH <sub>3</sub> CHO		HCOOH		CH <sub>3</sub> COOH		
					E	F	G	H	I	J	K	L	M
[C <sub>2</sub> H <sub>4</sub> ] <sub>0</sub> [ppmv]	7.97	4.01	2.03	4.16	4.12	4.10	4.09	4.04	4.05	4.18	4.09	4.09	4.02
[O <sub>3</sub> ] <sub>0</sub> [ppmv]	2.80	2.39	9.09	2.40	2.34	2.24	2.80	2.50	2.31	2.42	2.34	2.16	2.10
ΔC <sub>2</sub> H <sub>4</sub> [ppmv]	2.08	1.67	1.78	1.73	1.64	1.56	1.87	1.63	1.67	1.61	1.65	1.63	1.91
reaction time [min]	111	246	114	240	239	239	239	230	235	236	237	237	209
added compound [ppmv]					5	7.5	15	30	1	10	0.9	10	10
Y(ΔO <sub>3</sub> )	1.09	1.07	1.31	1.17	1.14	1.18	1.20	1.21	1.13	1.22	1.07	1.10	1.03
Y(HCHO)	0.92	0.91	0.77	n.d. <sup>c</sup>	0.73 <sup>d</sup>	0.62 <sup>d</sup>	0.51 <sup>d</sup>	n.d.	0.97	1.19	0.91	1.02	1.00
Y(CO)	0.29	0.30	0.44	n.d. <sup>c</sup>	0.47	0.50	0.56	n.d.	0.32	0.27	0.29	0.23	0.23
Y(CO <sub>2</sub> )	0.20	0.21	0.19	n.d. <sup>c</sup>	0.23	0.20	0.22	n.d.	0.29	0.41	0.23	0.28	0.26
Y(HCOOH)	0.04	0.04	0.04	n.d. <sup>c</sup>	0.18	0.21	0.35	0.58	0.05	0.06	-0.42	-0.91	0.04
Y(HPMF) <sup>e</sup> <sub>total</sub>	0.18	0.19	0.19	0.18	0.20	0.17	0.16	0.14	n.d.	n.d.	0.33	0.51	0.0
carbon balance	0.91	0.92	0.91	n.d.	1.00	0.94	0.98	n.d.	n.d.	n.d.	0.83	0.82	n.d.

<sup>a</sup> Product yields are denoted as Y(product) and represent the yield of product relative to ethene converted. <sup>b</sup> Experiment performed at a total pressure of 81 Torr. <sup>c</sup> Not determined because of pressure-dependent line shape. <sup>d</sup> Concentration of HCHO was determined by measuring the weak absorption of HCHO around 3471 cm<sup>-1</sup>. <sup>e</sup> HPMF<sub>total</sub> = HPMF + FAN (see text).

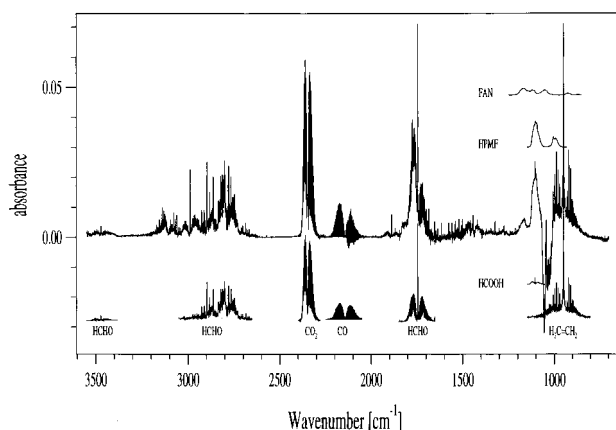
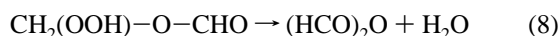


**Figure 2.** FTIR spectra used for evaluation of run B (see Table 1). Reference spectra of the products identified are shown with half the absorbance to which they contribute to the product spectra. Absorbance due to water vapor has been removed. The ozone absorption is negative since the background spectra were taken after O<sub>3</sub> was added.

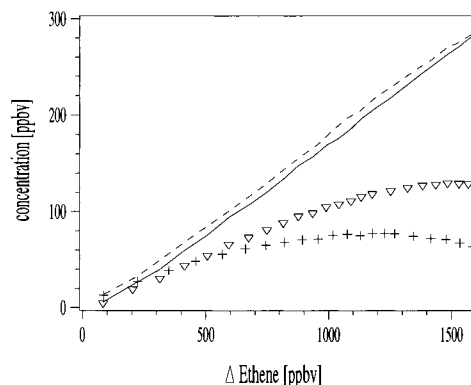
of ethene under varying initial concentrations are given in Table 1. Yields of the individual products are given relative to ethene consumption ( $[\text{product}]_t/[\text{ethene}]_0 - [\text{ethene}]_t$ ). Out of the products listed in Table 1, HCHO is formed in the decomposition of the primary ozonide (reaction 2) and CO (to a first approximation, see later), CO<sub>2</sub>, and HCOOH are formed from the decomposition/isomerization of the excited Criegee intermediate (reaction 4). HPMF is the only product which can be unambiguously attributed to a reaction of the stabilized Criegee intermediate:



Even though the structure of HPMF was unknown until some recent work,<sup>15</sup> this moderately stable product has also been observed in earlier studies on the gas phase ozonolysis of ethene<sup>4,24,25</sup> and was reported to decompose to formic anhydride (FAN) in a presumably heterogeneous process:

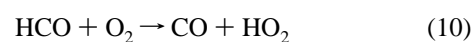
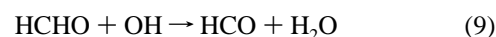


The heterogeneous nature of this process was confirmed in the present study. When the ozonolysis of ethene was carried out at a total pressure of 81 Torr while maintaining the concentrations of the reactants (as in the case of 730 Torr total pressure), a much faster decay of HPMF to FAN was observed (Figure 3).



**Figure 3.** Pressure dependence of the decomposition of HPMF. Experiments shown are run B and D from Table 1. Crosses are the concentration profiles of HPMF obtained at a total pressure of 81 Torr, and triangles are HPMF concentrations from the experiment at 730 Torr. Lines indicate HPMF<sub>total</sub> (= [HPMF] + [FAN]) of these two experiments.

In experiments where ethene was in excess of ozone, the increase in concentrations of all products (except HPMF and FAN) is linearly related to ethene conversion. To account for the time dependence of the HPMF yield, the expression  $[\text{HPMF}] + [\text{FAN}] = [\text{HPMF}]_{\text{total}}$  was used to characterize the amount of HPMF formed. Using excess ozone, the yield of HCHO decreases while the yield of CO increases with time. This can be explained by the reactions of the OH radical which is formed in the ozonolysis of ethene with an estimated 12% yield.<sup>10</sup> Under conditions of excess ethene, most of the OH radicals are scavenged by ethene. As a product of the ethene OH radical reaction, we observed 2-hydroxyethyl hydroperoxide (HOCH<sub>2</sub>-CH<sub>2</sub>OOH) in approximately 5% yield (unpublished results) in good agreement with data from Hatakeyama et al.<sup>26</sup> In experiment C (Table 1) the reactant ethene was eventually consumed by the reaction with excess ozone. In this case the OH radicals formed reacted with HCHO, yielding CO and HO<sub>2</sub> radicals, which in turn may react with O<sub>3</sub> to regenerate OH radicals:



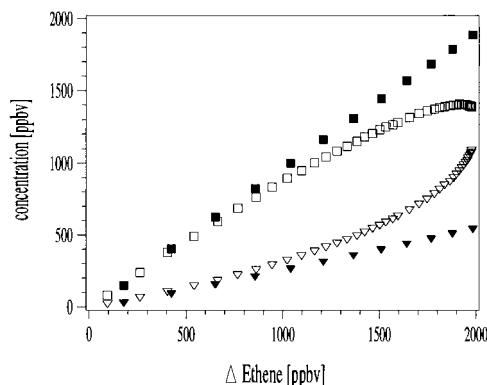


**Figure 4.** Comparison of CO and HCHO concentrations under different experimental conditions: Filled symbols are from run A (Table 1) performed with excess ethene; open symbols are from run C (Table 1) using excess ozone. Squares depict HCHO concentrations and triangles the concentrations of CO.

The relation between the decrease of HCHO and enhanced formation of CO due to the above reactions is shown in Figure 4, where data from runs A and C (Table 1) are displayed.

### Addition of HCHO

To elucidate the effect of HCHO on the product distribution, we performed experiments by adding various concentrations of HCHO while concentrations of the reactants were kept constant. Results are shown in Table 1 (runs E–H). Products, whose yields exhibit marked differences from those obtained in the absence of HCHO, are HCOOH and CO. The enhanced formation of these products, which was described also in earlier studies,<sup>7,27</sup> has been attributed to secondary reactions of HCHO with HO<sub>2</sub> and OH radicals. The reaction of HCHO and HO<sub>2</sub> involves a complex reaction scheme which introduces considerable uncertainty to the estimated extent of HCOOH formation via reaction 12.<sup>28,29</sup>



The change in the HPMF yields upon addition of HCHO provides the first indication of some reaction of HCHO with the stabilized Criegee intermediate CH<sub>2</sub>OO. In runs G and H, HCOOH concentrations reached 0.6–0.9 ppmv when yields were determined for the individual products. Though these concentrations of HCOOH are comparable with the initial HCOOH concentration in run K (Table 1), a decrease in HPMF formation was observed. From these results we come to the conclusion that some species, most likely HCHO, competes with HCOOH for the CH<sub>2</sub>OO intermediate. We examined the FTIR spectra of the experiments that were performed in the presence of HCHO in order to identify possible products from the reaction of CH<sub>2</sub>OO with HCHO. No absorbance that could not be attributed to one of the products listed in Table 1 was observed.

The enhanced formation of CO can be partially attributed to the reaction of HCHO with OH (reactions 9 and 10). However, the observed increase in CO yield from 29 to 30% (runs A, B in Table 1) to 47–56% in the presence of HCHO (runs E, F, and G, Table 1) is much too high to be explained solely by reaction 9. A comparison of the CO yields of runs A and B with experiments in the presence of species that are known to react with the stabilized Criegee intermediate (runs L, M)<sup>13</sup> suggests that part of the CO is not exclusively produced from the decomposition of the excited Criegee intermediate (reactions 4c, 4d) or reaction 9 but involves a reaction of the stabilized

**TABLE 2: Product Yields<sup>a</sup> in the Presence of H<sup>13</sup>CHO**

	A	B	C	D
[C <sub>2</sub> H <sub>4</sub> ] <sub>0</sub> [ppmv]	4.07	4.04	13.48	13.54
[O <sub>3</sub> ] <sub>0</sub> [ppmv]	2.55	2.30	7.83	8.49
ΔC <sub>2</sub> H <sub>4</sub> [ppmv]	1.62	1.46	5.60	5.68
[H <sup>13</sup> CHO] <sub>0</sub> [ppmv]	10	50	10	50
reaction time [min]	205	210	75	75
Y(ΔO <sub>3</sub> )	1.17	1.22	1.21	1.24
Y(H <sup>12</sup> CHO)	1.28	1.27	1.21	1.20
Y( <sup>12</sup> CO)	0.28	0.30	0.30	0.29
Y( <sup>13</sup> CO)	0.21	0.28	0.12	0.22
Y(H <sup>12</sup> COOH)	0.14	0.30	0.11	0.21
Y(H <sup>13</sup> COOH)	0.12	0.54	0.06	0.36

<sup>a</sup> Product yields are denoted as Y(product) and represent the yield of product relative to converted ethene.

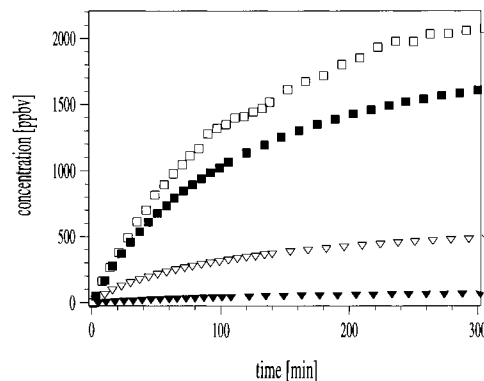


**Figure 5.** Increase of H<sup>12</sup>CHO and H<sup>12</sup>COOH concentrations in the presence of H<sup>13</sup>CHO. Open symbols are from run B (Table 2) performed in the presence of 50 ppmv H<sup>13</sup>CHO. Filled symbols are from run B (Table 1) without additional reaction partners. Triangles depict H<sup>12</sup>COOH concentrations and squares the concentrations of H<sup>12</sup>CHO.

Criegee intermediate. It seems therefore possible that CO is one of the products arising from the reaction of CH<sub>2</sub>OO and HCHO.

### Addition of H<sup>13</sup>CHO

A number of experiments with added H<sup>13</sup>CHO were performed in order to positively identify the products of the reaction of CH<sub>2</sub>OO with HCHO. Results are given in Table 2. Caused by the simultaneous formation of H<sup>13</sup>COOH and H<sup>12</sup>COOH, the <sup>13</sup>C-atom-containing isotopomers of HPMF and FAN were also formed in reactions 7 and 8. Due to spectral overlap in the region of the C–O stretching band and the absence of reference spectra, none of the isotopomers of HPMF or FAN were quantified in the experiments with added H<sup>13</sup>CHO.

The most important features of these experiments are the H<sup>12</sup>CHO yields which exceed 100% relative to ethene conversion and the enhanced formation of H<sup>12</sup>COOH. Figure 5 shows the increase in the yields of H<sup>12</sup>CHO and H<sup>12</sup>COOH compared to an experiment with similar initial concentrations of the educts but without addition of H<sup>13</sup>CHO. Since the only source of <sup>12</sup>C atoms that is available to bimolecular reactions is the stabilized Criegee intermediate, H<sup>12</sup>CHO and H<sup>12</sup>COOH must be considered as products arising from two independent reactions of H<sup>13</sup>CHO with CH<sub>2</sub>OO. First, reaction 13 was assumed to be relevant, leading to the formation of HCOOH and H<sup>13</sup>CHO:



The proposed reaction 13 leading to the formation of HCOOH was tested in two independent experiments where either 5 ppmv HCHO or 1 ppmv HCOOH was added. The observed ratio



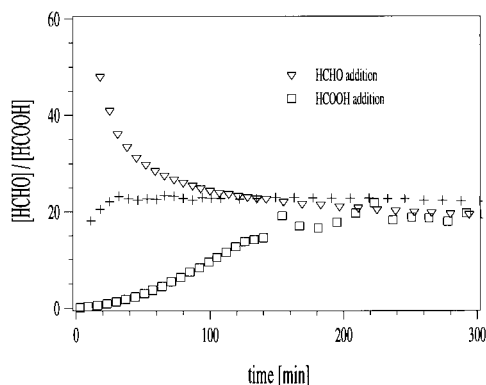


**Figure 6.** Ratio of [HCHO]/[HCOOH] in ethene ozonolysis. Initial concentrations of the experiments are given in Table 1 (runs B, E, G). Triangles correspond to run E (addition of HCHO), squares show data from run K (addition of HCOOH), and crosses indicate data from run B.

[HCHO]/[HCOOH] is plotted versus reaction time in Figure 6. In the early stage of the experiment with 5 ppmv HCHO addition (run E, Table 1), reaction 13 dominated over reaction 7, as can be seen from the enhanced formation of HCOOH. The formic acid subsequently competes with HCHO for the available  $\text{CH}_2\text{OO}$ , and the ratio [HCOOH]/[HCHO] remains constant. In the experiment with added HCOOH (run K, Table 1) the  $\text{CH}_2\text{OO}$  reacted only via reaction 7 until the concentration of HCOOH was reduced and the HCHO concentration formed in reaction 1 had built up. In experiments without additional reaction partners (runs A, B, Table 1) a similar value of [HCHO]/[HCOOH] is found throughout the reaction. These profiles are consistent with a reaction sequence producing HCOOH in reaction 13 and consuming HCOOH in reaction 7, implying that  $k_7/k_{13} \approx [\text{HCHO}]/[\text{HCOOH}] = 20 \pm 4$ .

To account for the formation of  $\text{H}^{12}\text{CHO}$  in the presence of  $\text{H}^{13}\text{CHO}$ , two possible reactions can be formulated which also enable us to explain the increased amount of  $^{13}\text{CO}$  in the presence of  $\text{H}^{13}\text{CHO}$ :



From reactions 13 and 14, which have been suggested to explain the enhanced formation of  $^{13}\text{CO}$ ,  $\text{H}^{12}\text{COOH}$ , and  $\text{H}^{12}\text{CHO}$  in ethene ozonolysis in the presence of  $\text{H}^{13}\text{CHO}$ , it is apparent that some exchange of C isotopes has taken place. In the current notation of reaction 13,  $\text{H}^{13}\text{CHO}$  merely acts as a catalyst for the isomerization of the  $\text{CH}_2\text{OO}$  intermediate. Reaction 14, on the other hand, can be described as the decomposition of the  $\text{CH}_2\text{OO}$  intermediate after exchange of the C atom with  $\text{H}^{13}\text{CHO}$ . This behavior can be rationalized by assuming a cyclic adduct, which may either stabilize to give secondary ozonides or decompose into smaller fragments. The secondary ethene ozonide has not been observed in the gas phase, but upon addition of carbonyl compounds other than HCHO the corresponding secondary ozonides were reported as products.<sup>4,20</sup> We therefore propose that the excited secondary ethene ozonide is formed according to reaction 3' and then decomposes, presumably due to a lack of collisional stabilization, to yield HCHO, HCOOH, and CO as stable products via reactions 13, 14a, and 14b. The assumption that a secondary ethene ozonide is formed opens a convenient way to explain the formation of both  $\text{H}^{12}\text{CHO}$  and  $\text{H}^{12}\text{COOH}$  from reaction

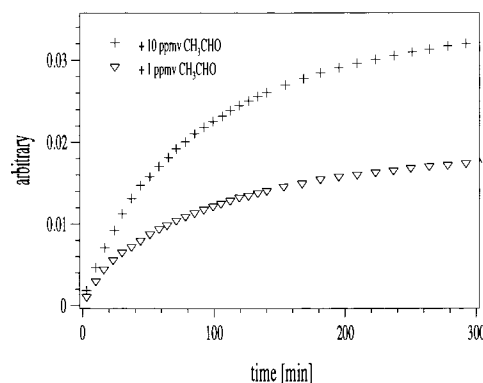
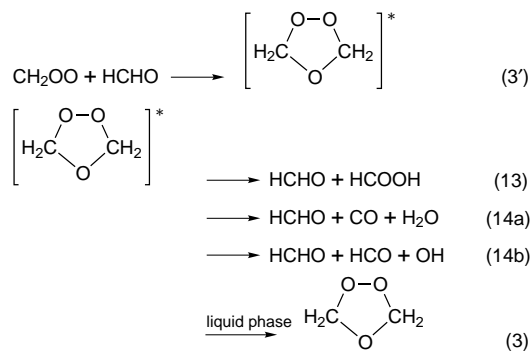


**Figure 7.** Absorption of the secondary propene ozonide at  $1123 \text{ cm}^{-1}$ . Triangles and crosses are from experiments in the presence of 1 and 10 ppmv  $\text{CH}_3\text{CHO}$ , respectively (runs I, J, Table 1).

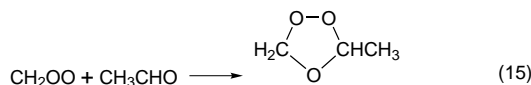
13, because the excited secondary ethene ozonide, being a symmetrical entity, scrambles the isotopic signature of its C atoms.



It is interesting to note that in the ethene ozonolysis in the liquid phase HCOOH and HCHO were observed as minor volatile products, whereas secondary ethene ozonide was the main product,<sup>17</sup> indicating that the intermediates formed in liquid phase ozonolysis were not exclusively stabilized.

#### Addition of $\text{CH}_3\text{CHO}$

Unlike the secondary ethene ozonide, which has not been observed, the addition of carbonyl compounds other than HCHO has been reported to yield the corresponding secondary ozonides in the gas phase.<sup>20,30</sup> In experiments where  $\text{CH}_3\text{CHO}$  was added to the ethene–ozone system, the formation of secondary propene ozonide was observed (runs I, J, Table 1). The propene ozonide, exhibiting a strong absorption at  $1123 \text{ cm}^{-1}$ , was identified by comparison with a reference spectrum (courtesy of Dr. Hatakeyama).



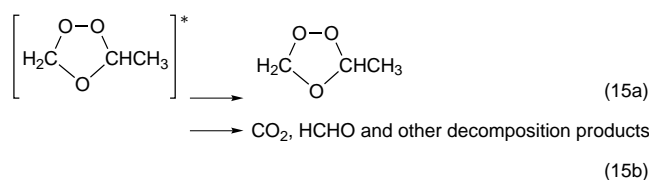
Secondary propene ozonide was formed with a constant yield and was stable under experimental conditions. The temporal profiles of its absorption at  $1123 \text{ cm}^{-1}$  are shown in Figure 7. Apart from the formation of secondary propene ozonide, the obtained product yields of HCHO and  $\text{CO}_2$  were increased markedly compared to experiment B (Table 1). The increase of both  $\text{CO}_2$  and HCHO yields by  $\approx 20\%$  cannot be attributed to the oxidation of  $\text{CH}_3\text{CHO}$  by the OH radical. Under the experimental conditions of run J (Table 1) and an OH yield of 12%,<sup>10</sup> most of the OH radicals formed will react with ethene,

TABLE 3: Branching Ratios of the CH<sub>2</sub>OO\* Intermediate

	Su et al. <sup>4</sup>	Atkinson et al. <sup>33</sup>	Horie and Moortgat <sup>7</sup>	Thomas et al. <sup>8</sup>	this work
CH <sub>2</sub> OO* → CO <sub>2</sub> + H <sub>2</sub>	} 0.22	0.13	0.13	0.13	} 0.23
→ CO <sub>2</sub> + 2 H		0.06	0.09	0.09	
→ CO + H <sub>2</sub> O	} 0.36	0.44	0.31	0.31	} 0.23
→ HCO + OH		0	0	0	
→ HCOOH	0.04	0	0	0.03	0.04
CH <sub>2</sub> OO* + M → CH <sub>2</sub> OO	0.38	0.37	0.47	0.44	0.50

and the maximum CO<sub>2</sub> yield from OH-radical-initiated CH<sub>3</sub>-CHO oxidation can be expected to be 5%.

No information is available as to whether the formation of secondary propene ozonide (reaction 15) is the only reaction of the CH<sub>2</sub>OO intermediate with CH<sub>3</sub>CHO or if decomposition channels analogous to reaction 14 exist. Taking into account that all secondary ethene ozonide decomposes, it seems plausible that the presence of an additional methyl group does not result in a complete stabilization. Assuming therefore that the product of reaction 15 also possesses some excess internal energy, the enhanced CO<sub>2</sub> and HCHO yields might be explained by the partial decomposition of the secondary propene ozonide:



Decomposition of secondary ozonides following pyrolysis or photolysis<sup>31,32</sup> has shown to proceed via the cleavage of the peroxidic O–O bond. In thermal decomposition ( $\Delta E \approx 0.8 \text{ kJ mol}^{-1}$ ) the major products were found to be the corresponding acids and carbonyl compounds.<sup>31</sup> In the photolysis of secondary propene ozonide<sup>32</sup> HCHO and CO<sub>2</sub> were additionally detected as products. These results cannot be used directly to characterize the products of the decomposition of an excited secondary ozonide, such as formed in reaction 15. However in the case of the ethene–ozone–CH<sub>3</sub>CHO system, the intermediate formation of an excited acetic acid, which fragments into CH<sub>3</sub> and COOH radicals yielding further CO<sub>2</sub> and HCHO as stable products, may be visualized as a plausible mechanism.

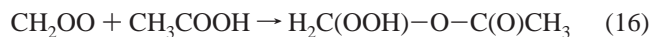
### Branching Ratios of the Excited CH<sub>2</sub>OO\* Decomposition

Except for the experiments in the presence of HCHO, ethene is not exclusively consumed by the reaction with ozone, but also, though to a minor extent, by reaction with OH radicals. As a consequence, the evaluated yields, which were determined relative to ethene consumption, do not correspond directly to branching ratios. The experimentally determined OH radical yield is 12%,<sup>10</sup> and in the presence of excess ethene, OH radicals are expected to react predominantly with ethene. Based on the results of Atkinson et al.,<sup>10</sup> which are in good agreement with results of this study (see below), product yields were multiplied by a factor of 1.1 in order to determine the branching ratios for the individual decomposition or isomerization reactions. The alternative approach would be to express yields relative to ozone consumption. This was considered, but rejected because ozone has additional sinks via reaction 11 and the decomposition of ozone at the reactor wall. The unimolecular rate constant of ozone decomposition was determined in separate experiments and was about  $3.5 \times 10^{-6} \text{ s}^{-1}$ .

Previously, all the CO produced has been assumed to be due to unimolecular decomposition of CH<sub>2</sub>OO\*, reactions 4c and 4d. The present study clearly shows that a fraction of CO is

produced in a bimolecular reaction of the stabilized CH<sub>2</sub>OO via reaction 14a or 14b followed by reaction 10. To a first approximation, the fraction of CO that is solely produced from CH<sub>2</sub>OO\* decomposition is readily available from the data of run L (Table 1), where all the CH<sub>2</sub>OO is consumed by HCOOH, and hence reaction 14 should be of negligible influence. Some uncertainty exists about this value due to the possible formation of CO via reactions 9 and 10. We estimate this contribution to be about 0.02 under the experimental conditions, based on the initial reactant concentrations and the rate constants for the OH reaction. Therefore we estimate the branching ratio for reactions 4c + 4d  $\approx (0.23 - 0.02) \times 1.1 = 0.23$ .

The branching ratio for the HCOOH formation 4e can be estimated from the data obtained in the presence of added CH<sub>3</sub>COOH (run M, Table 1). Under these conditions, HCOOH formation by reaction 13 is completely suppressed, due to the dominance of the reaction between the CH<sub>2</sub>OO intermediate and CH<sub>3</sub>COOH:<sup>13</sup>



Thus the obtained yield for HCOOH in this experiment can be used to calculate the branching ratio for 4e, which equals  $0.04 \times 1.1 = 0.04$ . The average CO<sub>2</sub> yield of 0.21 results in a branching ratio for reactions 4a + 4b of  $0.21 \times 1.1 = 0.23$ , which is in good agreement with published results (see Table 3). The extent of the stabilization reaction 3 can be derived by assuming that all Criegee intermediates that do not decompose by reaction 4 will be thermalized. With the above quantification of the different branching ratios 4a to 4e, the degree of stabilization  $k_5M/(k_4 + k_5M)$  can be set to 0.50, which is slightly higher than values from the literature. A similar result is obtained from experiment L (Table 1) in the presence of 10 ppmv HCOOH, where it is expected that the CH<sub>2</sub>OO intermediate exclusively reacts with the excess HCOOH (reaction 7). Under these conditions the yield of HPMF<sub>total</sub> was determined as 0.51, indicating that the quantification of HPMF, although solely based on the comparison of typical band strength at 1760 cm<sup>-1</sup>, is fairly accurate.

Results for the branching ratio of reactions 4a to 4e are compared to values from literature in Table 3. In our study, part of the CO formed was identified as a product of reaction 14, hence leading to a smaller branching ratio of reactions 4c + 4d and an increased degree of stabilization. Furthermore, the results of the study of Su et al.<sup>4</sup> and the review article of Atkinson<sup>33</sup> were based on experiments that were made with initial ozone concentrations equal to or exceeding the amount of ethene in the system and thus giving rise to CO formation by oxidation of HCHO (reactions 9 and 10).

### Branching Ratio for the Reaction of CH<sub>2</sub>OO with HCHO

The branching ratio for reactions 13 and 14 can be deduced from the HCOOH and CO budget in experiment B (Table 1). In this experiment the only relevant HCOOH sources are the decomposition of the excited Criegee intermediate (reactions 4e, 13). Since the total amount of HCOOH formed equals

**TABLE 4: Mechanism of C<sub>2</sub>H<sub>4</sub> Ozonolysis in the Gas Phase**

(i) Primary Reactions			
(1)	C <sub>2</sub> H <sub>4</sub> + O <sub>3</sub>	→ Primary ozonide	
(2)	Primary ozonide	→ CH <sub>2</sub> OO* + HCHO	
(ii) Branching Ratio of CH <sub>2</sub> OO*			
(4a)	CH <sub>2</sub> OO*	→ CO <sub>2</sub> + H <sub>2</sub>	} 0.23
(4b)		→ CO <sub>2</sub> + 2 H	
(4c)		→ CO + H <sub>2</sub> O	} 0.23
(4d)		→ HCO + OH	
(4e)		→ HCOOH	} 0.04
(5)	CH <sub>2</sub> OO* + M	→ CH <sub>2</sub> OO + M	
(iii) Fate of the Stabilized CH <sub>2</sub> OO in C <sub>2</sub> H <sub>4</sub> /O <sub>3</sub> System Considering 50% Yield			
(13)	CH <sub>2</sub> OO + HCHO	→ HCOOH + HCHO	} 0.22
(14a)		→ HCHO + H <sub>2</sub> O + CO	
(14b)		→ HCHO + HCO + OH	} 0.07
(7)	CH <sub>2</sub> OO + HCOOH	→ CH <sub>2</sub> (OOH)-O-CHO	
(8)	CH <sub>2</sub> (OOH)-O-CHO	→ (HCO) <sub>2</sub> O + H <sub>2</sub> O	} 0.21

<sup>a</sup> The relative importance of the reactions of the CH<sub>2</sub>OO intermediate is valid only in the absence of added reaction partners for the CH<sub>2</sub>OO intermediate (runs A–C in Table 1). Also the subsequent reactions of the HO<sub>2</sub> and OH radicals, which are produced in the presence of oxygen, are omitted from this table.

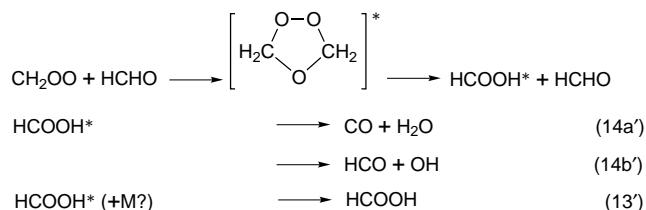
[HPMF + FAN + HCOOH], the overall production of HCOOH due to reaction 13 can be estimated to be

$$Y_{R13} = Y_{HPMF} + Y_{FAN} + Y_{HCOOH} - Y_{R4e} \approx 0.19$$

where  $Y_{RX}$  corresponds to the conversion of reaction X relative to the reaction of ethene and O<sub>3</sub> (reaction ) and  $Y_Z$  stands for the yield of an arbitrary product Z. The amount of CO from reaction 14 can likewise be determined from the change in the CO yield due to the addition of HCOOH (experiments B and L, Table 1). In terms of CO production, the only difference is the suppression of reaction 14 by reaction 7; hence the CO production in experiment B from reaction 14 is about 0.07. Combining the information obtained from the CO and the HCOOH budget, the branching ratio of  $k_{13}/k_{14} = 0.19/0.07 \approx 3:1$ . The relative importance of reactions 7, 13, and 14 in an ozonolysis, where no additional reaction partners for the stabilized Criegee intermediate were added, is shown in Table 4. Since in the ethene–ozone system part of the ethene is consumed by OH radicals, the rates for reactions with the stabilized Criegee intermediate given in Table 4 are normalized to a 50% formation of this species.

According to the results of this study, the reaction between the CH<sub>2</sub>OO intermediate and HCHO might represent another, previously not considered, route to form OH radicals. The extent of OH radicals that might be produced from this reaction (7%, see above discussion) is in good accordance with the overall (including reaction 11) OH yield reported by Gutbrod et al.<sup>11</sup> and Atkinson et al.<sup>10</sup> While there is ample experimental evidence for the formation of OH radicals in the ethene ozonolysis, recent theoretical studies<sup>11,34</sup> arrived at different results concerning the possibility that reaction 4d leads to OH radical formation. Donahue et al.<sup>34</sup> came to the conclusion that, on the basis of *ab initio* calculations, reaction 4d is the most likely origin of the OH radicals observed directly by a LIF system. In a recent study dealing with the energetics of the Criegee intermediate CH<sub>2</sub>OO,<sup>11</sup> it was concluded that the dissociation of the CH<sub>2</sub>OO intermediate is not likely to yield HCO and OH (reaction d) since it involves the transitory formation of a carbene, which is unfavorable. However the formation of CO as a stable product from the reaction of the stabilized Criegee intermediate with HCHO can also be explained by the partial fragmentation of excited HCOOH,

which is formed as the primary product in the decomposition of the secondary ethene ozonide.



In this presentation the experimentally observed OH radicals<sup>10</sup> may be explained straightforwardly by the decomposition of HCOOH\*, without the direct involvement of a stabilized Criegee intermediate. Although this mechanism seems to be a plausible way of explaining the formation of OH radicals, neither our experimental data nor theoretical work enables us to distinguish between the different possibilities of the OH formation discussed above. The question whether OH radicals are formed unimolecularly or bimolecularly is of interest for atmospheric chemistry since reaction 14b is of no importance under tropospheric conditions, whereas the branching ratios of the reactions 4a–4e remain unaffected.

It should be pointed out that the above discussion cannot easily be extended to the reactions of Criegee intermediates other than CH<sub>2</sub>OO. OH radicals that are formed in ozonolysis of alkenes other than ethene<sup>10,35</sup> are believed to result from unimolecular decay of the excited Criegee intermediate, which proceeds via  $\beta$ -hydrogen atom abstraction from the Criegee intermediate.<sup>36</sup>

## Conclusions

Our finding that the reaction of the Criegee intermediate with HCHO proceeds via some cyclic adduct enables us to draw some general conclusions about the similarities of the ozonolysis of ethene in the liquid and the gas phase. In both phases, the stabilized Criegee intermediate is formed and reacts in the same manner with both hydroxy and carbonyl compounds.

All differences in the observed product distribution can be attributed to the less efficient stabilization in the gas phase. Although no quantitative studies on the extent of decomposition of the Criegee intermediate in the liquid phase exist, this pathway seems to be of minor importance, as can be judged from the measured yield of the secondary ozonides (up to 80%), observed as main products.<sup>17</sup> For the gas phase it was shown that the degree of stabilization is pressure dependent, leveling off at about 400 Torr.<sup>37</sup> For the secondary ethene ozonide, the results of this study indicate that it is unstable in the gas phase, presumably due to lack of collisional stabilization. The secondary propene ozonide formed in the presence of CH<sub>3</sub>CHO (reaction 5) appears to decompose only partially, presumably stabilized by having more vibrational degrees of freedom.

The apparent discrepancies between the liquid and the gas phase ozonolysis can therefore be largely attributed to the different foci of the various studies. Whereas liquid phase ozonolysis is largely carried out to observe reactions of the stabilized Criegee intermediate, gas phase studies tend to focus on small product molecules originating from the decomposition of the Criegee intermediate, with a special emphasis on the production of free radicals, namely, OH radicals. The interest in the comparatively small molecules (e.g., CO, CO<sub>2</sub>, HCHO) reflects also the complications arising from the simultaneous formation of free radicals and the analytical complications due

to the generally much lower concentrations employed in gas phase studies.

The reaction of HCHO with the stabilized Criegee intermediate CH<sub>2</sub>OO represents a major HCOOH source under the conditions of this study, but is of minor importance (if at all) to the atmosphere. In a recent study from our laboratory<sup>14</sup> the main product of the reaction of CH<sub>2</sub>OO with H<sub>2</sub>O (the most important atmospheric reaction partner) has been found to be hydroxymethyl hydroperoxide (HOCH<sub>2</sub>OOH) (reaction 7). The rate constant for reaction 17 was found to be 14 000 times smaller than the rate constant for the reaction of CH<sub>2</sub>OO with HCOOH.



Under tropospheric conditions where H<sub>2</sub>O concentrations are on the order of 10<sup>4</sup> ppmv, reactions with HCOOH and HCHO cannot therefore be expected to compete with the formation of HOCH<sub>2</sub>OOH.

**Acknowledgment.** The authors gratefully acknowledge the support of this work by the Deutsche Forschungsgemeinschaft (DFG) through Sonderforschungsbereich 233 “Dynamics and Chemistry of Hydrometeors” and the European Community through the research grant LABVOC (EV5V\_CT91\_0038). P.N. would like to thank Abraham Horowitz for helpful discussions.

## References and Notes

- Atkinson, R. *J. Phys. Chem. Ref. Data* **1994**, *2*, 1–216.
- Atkinson, R. *J. Phys. Chem. Ref. Data* **1997**, *26*, 215–290.
- Criegee, R. *Angew. Chem.* **1975**, *87*, 765–771, and references cited therein.
- Su, F.; Calvert, J. G.; Shaw, J. H. *J. Phys. Chem.* **1980**, *84*, 239–246.
- Hatakeyama, S.; Akimoto, H. *Res. Chem. Intermed.* **1994**, *20*, 503–524.
- Herron, J. T.; Huie, R. E. *J. Am. Chem. Soc.* **1977**, *99*, 5430–5435.
- Horie, O.; Moortgat, G. K. *Atmos. Environ.* **1991**, *25A*, 1881–1896.
- Thomas, W.; Zabel, F.; Becker, K. H.; Fink, E. H. A mechanistic study on the ozonolysis of ethene. *Physicochemical behaviour of atmospheric pollutants*; Varese, Italy, 1993; pp 207–212.
- Martinez, R. I.; Herron, J. T.; Huie, R. E. *J. Am. Chem. Soc.* **1981**, *103*, 3807–3820.
- Atkinson, R.; Aschmann, S. M.; Arey, J.; Shorees, B. *J. Geophys. Res.* **1992**, *97*, 6065–6073.
- Gutbrod, R.; Schindler, R. N.; Kraka, E.; Cremer, D. *Chem. Phys. Lett.* **1996**, *252*, 221–229.
- Atkinson, R.; Lloyd, A. *J. Phys. Chem. Ref. Data* **1984**, *13*, 315–444.
- Neeb, P.; Horie, O.; Moortgat, G. K. *Int. J. Chem. Kinet.* **1996**, *28*, 721–730.
- Neeb, P.; Sauer, F.; Horie, O.; Moortgat, G. K. *Atmos. Environ.* **1997**, *31*, 1417–1423.
- Neeb, P.; Horie, O.; Moortgat, G. K. *Chem. Phys. Lett.* **1995**, *246*, 150–156.
- Thamm, J.; Wolff, S.; Turner, W. V.; Gäb, S.; Thomas, W.; Zabel, F.; Fink, E. H.; Becker, K. H. *Chem. Phys. Lett.* **1996**, *258*, 155–158.
- Fong, G. D.; Kuczkowski, R. L. *J. Am. Chem. Soc.* **1980**, *102*, 4763–4768.
- Fajgar, R.; Vitek, J.; Haas, Y.; Pola, J. *Tetrahedron. Lett.* **1996**, *37*, 3391–3394.
- Griesbaum, K.; Miclaus, V.; Jung, I. C. *Environ. Sci. Technol.* **1998**, *32*, 647–649.
- Neeb, P.; Horie, O.; Moortgat, G. K. *Tetrahedron Lett.* **1996**, *37*, 9297–9300.
- Finkbeiner, M.; Neeb, P.; Horie, O.; Moortgat, G. K. *Fresenius J. Anal. Chem.* **1995**, *351*, 521–525.
- Muramatsu, I.; Itioi, M.; Tsuji, M.; Hagitani, A. *Bull. Chem. Soc. Jpn.* **1964**, *37*, 756.
- DeMore, W. B.; Sander, S. P.; Howard, C. J.; Ravishankara, A. R.; Golden, D. M.; Kolb, C. E.; Hampson, R. F.; Kurylo, M. J.; Molina, M. J. *JPL Publication 92-20*, 1992.
- Kan, C. S.; Su, F.; Calvert, J. G.; Shaw, J. H. *J. Phys. Chem.* **1981**, *85*, 2359–2363.
- Niki, H.; Maker, P. D.; Savage, C. M.; Breitenbach, L. P. *J. Phys. Chem.* **1981**, *85*, 1024–1027.
- Hatakeyama, S.; Lai, H.; Murano, K. *Environ. Sci. Technol.* **1995**, *29*, 3–835.
- Horie, O.; Moortgat, G. K. Ozonolysis of alkenes under atmospheric conditions. In *Ozone in the atmosphere*; Boikov, R. D., Fabian, P., Eds.; DEEPAK Publishing: 1989; pp 698–701.
- Su, F.; Calvert, J. G.; Shaw, J. H. *J. Phys. Chem.* **1979**, *83*, 3185–3191.
- Veyret, B.; Lesclaux, R.; Rayez, M.-T.; Tyndall, G. S.; Cox, R. A.; Moortgat, G. K. *J. Phys. Chem.* **1989**, *93*, 2368–2374.
- Niki, H.; Maker, P. D.; Savage, C. M.; Breitenbach, L. P. *Chem. Phys. Lett.* **1977**, *46*, 327–330.
- Story, P. R.; Hall, T. K.; Morrison, W. H. I.; Farine, J.-C. *Tetrahedron Lett.* **1968**, *52*, 5397–5400.
- Hatakeyama, S.; Akimoto, H. *Bull. Chem. Soc. Jpn.* **1983**, *56*, 655–656.
- Horie, O. *Atmos. Environ.* **1990**, *24A*, 1–41.
- Donahue, N. M.; Kröll, J. H.; Anderson, J. G.; Demerjian, K. L. *Geophys. Res. Lett.* **1998**, *25*, 59–62.
- Atkinson, R.; Aschmann, S. M. *Environ. Sci. Technol.* **1993**, *27*, 1357–63.
- Niki, H.; Maker, P. D.; Savage, C. M.; Breitenbach, L. P.; Hurley, M. D. *J. Phys. Chem.* **1987**, *91*, 941–946.
- Hatakeyama, S.; Kobayashi, H.; Akimoto, H. *J. Phys. Chem.* **1984**, *88*, 4736–4739.